Journal of Power Sources 238 (2013) 48–52

Contents lists available at SciVerse ScienceDirect

Journal of Power Sources

journal homepage: www.elsevier.com/locate/jpowsour

Short communication

Structure and transport properties of $Li_7La_3Zr_{2-0.75x}Al_xO_{12}$ superionic solid electrolytes

A.A. Raskovalov*, E.A. Il'ina, B.D. Antonov

Institute of High-Temperature Electrochemistry, Ural Branch of RAS, Ekaterinburg, Russia

HIGHLIGHTS

- We prepared $Li_7La_3Zr_{2-0.75x}Al_xO_{12}$ (x = 0.00, 0.05, 0.10, 0.15, 0.20, 0.25, 0.30) by the citrate–nitrate method.
- We studied phase composition and conductivity of $Li_7La_3Zr_{2-0.75x}Al_xO_{12}$.
- We found that the composition with x = 0.15 has high total conductivity, 3.4 × 10^{-4} S cm^{-1}, at 25 °C.
- We obtained cubic modification of $Li_7La_3Zr_2O_{12}$ by treatment at 1150 °C for 1 h.

ARTICLE INFO

Article history:
Received 31 October 2012
Received in revised form
11 March 2013
Accepted 12 March 2013
Available online 21 March 2013

Keywords:
LLZ
Li-ion conductivity
Phase composition
Solid electrolyte

ABSTRACT

Samples of $Li_7La_3Zr_{2-0.75x}Al_xO_{12}$ (x = 0.00, 0.05, 0.10, 0.15, 0.20, 0.25, 0.30) were synthesised using the citrate–nitrate method. The crystal structure of each sample was characterised using X-ray diffraction. Doping the samples with Al reduced the synthesis time. The cubic modification of $Li_7La_3Zr_2O_{12}$ was obtained by treatment at 1150 °C for 1 h. The conductivity of the ceramic samples was studied by complex impedance spectroscopy at 25–230 °C. The composition with x = 0.15 had the highest total conductivity, $3.4 \cdot 10^{-4}$ S cm^{-1}, at 25 °C.

1. Introduction

Most lithium-ion rechargeable batteries contain liquid electrolytes, which have some disadvantages, one of which is flammability. A current direction in scientific research is the development of solid electrolytes for lithium power sources, which could improve not only the ionic conductivity but also the stability of cathode materials and lithium metal.

$Li_7La_3Zr_2O_{12}$ (LLZ) is a promising solid electrolyte for application in all-solid-state lithium-ion batteries. The tetragonal modification of LLZ is thermodynamically stable relative to lithium metal, but it has low conductivity at room temperature ($\sim 10^{-7}$ S cm^{-1}) [1]. The cubic phase of this compound has higher conductivity and is also stable relative to lithium metal [2]. However, there are contradictions in the literature on the tetragonal to cubic phase transition temperature. Adams and Rao [3] reported the phase transition temperature of 177 °C according to an X-ray diffraction (XRD) study, while Kokal et al. [4] showed using DSC that the phase transition temperature is much higher (approximately 700 °C).

At the same time, numerous experiments have revealed that only long-term exposure to high temperatures can stabilise the cubic phase of LLZ (1150 °C for 35 h [5], 1180 °C for 36 h [6,7], and 1230 °C for 36 h [8]). Furthermore, it has been demonstrated that lithium oxide can evaporate from samples [2,5,6]. Improved conditions for obtaining the cubic phase can be achieved by doping the material. In work [9], the synthesis time was reduced to 6 h at 1200 °C by adding Al_2O_3 to the initial reagents.

It is also known that substitution of Al for tetravalent cations in solid electrolytes enhances electrolyte conductivity. For example, the replacement of Ti^{4+} by Al^{3+} in $LiTi_2(PO_4)_3$ increases conductivity from $1 \cdot 10^{-4}$ to $9 \cdot 10^{-2}$ S cm^{-1} at 300 °C [10]. Most likely, the ionic conductivity of LLZ can be improved by replacement of zirconium by aluminium cations.

The authors of works [9,11] added Al to LLZ and assumed that aluminium occupies the lithium positions in the structure. However,

* Corresponding author. Tel.: +7 343 362 31 81; fax: +7 343 374 59 92.
E-mail address: other@e1.ru (A.A. Raskovalov).

0378-7753/$ – see front matter © 2013 Elsevier B.V. All rights reserved.
http://dx.doi.org/10.1016/j.jpowsour.2013.03.049

it was previously shown [3] that the stabilisation of the cubic phase occurs when the zirconia sublattice is doped with pentavalent cations. Moreover, some researchers believe that Al can substitute for Zr or even for La [12]. Therefore, the position of aluminium in the LLZ structure is still unclear. In our study, we tried to insert Al into Zr positions in LLZ to reveal changes in the properties of this system.

2. Experimental

Samples of $Li_7La_3Zr_{2-0.75x}Al_xO_{12}$ with $x = 0.00$, 0.05, 0.10, 0.15, 0.20, 0.25, 0.30 and $Li_xLa_3Zr_2O_{8.5+0.5x}$ ($x = 7$, 8, 9) have been synthesised. Li_2CO_3, La_2O_3, $Al(NO_3)_3 \cdot 9H_2O$, and an aqueous solution of $ZrO(NO_3)_2$ were used as precursors for citrate–nitrate synthesis. These components were dissolved in a mixture of dilute nitric and citric acid. The resulting solution was evaporated at 80 °C to form a transparent gel. The gel was then dried and pyrolysed at ~200 °C, which resulted in the formation of black powder. The synthesis was performed by stepwise increasing of temperature from 700 °C to 900 °C for 5 h, at the final temperature calcinations for 1 h. After each stage of synthesis, the mixture of reagents was thoroughly ground in an agate mortar.

The synthesised powder of LLZ (designated as "powder") was examined by XRD with a Rigaku D-MAX-2200V diffractometer at room temperature. A curved graphite crystal was used to monochromate CuK_α radiation. The data were collected over a 2θ range of 10–70° in continuous mode at a scan rate of 3 ° min^{-1}.

Neutron diffraction measurements of $Li_xLa_3Zr_2O_{8.5+0.5x}$ ($x = 7$, 8, 9) at room temperature were performed on the high-resolution powder diffractometer D7a at the research reactor IVV-2M of the Institute of Metal Physics, Urals Branch of the Russian Academy of Sciences. Powdered samples were sealed in cylindrical vanadium containers with diameters of 8 mm The D7a diffractometer used the double graphite (0 0 2)–Ge (5 1 1) monochromator; the neutron wavelength l was 1.5321 Å. Neutron diffraction patterns were recorded in the scattering angle ranges 10–125° with a step of 0.05°. Profile refinements of the diffraction patterns were made by Rietveld analysis using the FULLPROF program.

The pellets of LLZ were pressed at 160 MPa and annealed at 1150 °C for 1 h. The samples obtained from this process (designated as "annealed samples") were ground and studied by X-ray analysis as described above. Processing of XRD patterns, determination of the phase composition and structural parameters were performed using Jade 6 software and the PDF-2 database.

For AC impedance studies, both sides of the annealed samples were painted with gallium–silver electrode paste. The impedance measurements were performed in air at temperatures ranging from 25 to 230 °C, using a LCR-meter 819 (Goodwill Instruments) in the 0.012–100 kHz frequency range and a two-probe cell with silver electrodes. The results were fitted using mathematical modelling. All of the conductivity measurements were performed on two sets of identical samples to check the reproducibility of the results.

3. Results and discussion

3.1. The phase composition and structural parameters

The XRD patterns of the powders obtained after synthesis (final annealing at 900 °C) are shown in Fig. 1.

According to our analysis, most of the XRD peaks correspond to the LLZ tetragonal phase. At $x \leq 0.15$, only peaks of the tetragonal LLZ are presented. The samples with a higher aluminium content ($x > 0.15$) contain an impurity phase of $LaAlO_3$. We therefore suggest that Al should substitute for Zr in the LLZ structure at aluminium concentrations <0.15. Further doping leads to liberation of the second phase, i.e., a large addition of aluminium does not

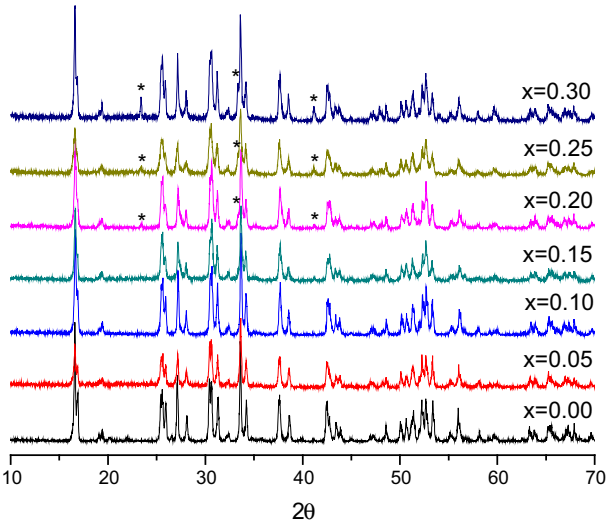

Fig. 1. XRD patterns of $Li_7La_3Zr_{2-0.75x}Al_xO_{12}$ powders ($x = 0.00$, 0.05, 0.10, 0.15, 0.20, 0.25, 0.30) (* – $LaAlO_3$).

allow the material to maintain the LLZ structure. The structure of $LaAlO_3$ represents a network of AlO_6 octahedra with La ions between them [13], similar to the structure of LLZ [1] with lanthanum and lithium atoms between ZrO_6 octahedra (Fig. 2). As the structure of $LaAlO_3$ is similar to that of LLZ, with Al atoms replacing the Zr atoms, we assume that the aluminium atoms in $LaAlO_3$ occupy the positions of zirconium in LLZ. The La–O bond lengths are similar in both compounds (2.50 Å for LLZ and 2.53 Å for $LaAlO_3$), while the Al–O bond length in $LaAlO_3$ is much shorter (1.899 Å) than the Zr–O bond length in LLZ (~2.11 Å). For this reason, it is likely that the solid solutions are formed only at low concentrations of aluminium. Because Al ions escape from the LLZ structure in equal ratio with La ions escaping from the $LaAlO_3$ phase, it is unlikely that aluminium occupies the positions of lanthanum.

Because the cubic phase was not obtained after annealing at 900 °C, the powder was pressed into pellets and annealed at higher temperature (1150 °C) (Experimental section). The XRD patterns of the annealed samples are presented in Fig. 3. The diffraction peaks of the sample without Al correspond to the tetragonal modification of LLZ. We therefore conclude that no cubic phase is stabilised in the undoped LLZ because our annealing conditions are milder than those in works [5–7]. According to the XRD data, addition of aluminium leads to the stabilisation of the cubic phase. The cubic modification of LLZ can be obtained by thermal treatment at 1150 °C for 1 h versus the 6 h that was demonstrated in Ref. [9]. There is a possibility that some aluminia from the crucible is uncontrollably incorporating into the sample, but in work [8], it was demonstrated that even under more extreme conditions (1230 °C for 36 h), the incorporation of aluminium quite low (<2%). We therefore believe that in the present work, the composition is close to our initial formulation.

In the $Li_7La_3Zr_{2-0.75x}Al_xO_{12}$ series, there is only one single-phase composition at $x = 0.15$. Although $LaAlO_3$ is present in the powder of Al-doped LLZ with $x \geq 0.20$ before annealing, this phase is absent in the annealed sample with $x = 0.20$. Most likely, at high temperatures, the lithium oxide evaporates from LLZ [2] and interacts with lanthanum aluminate, giving rise to lanthanum–lithium aluminate by the reaction:

$$2LaAlO_3 + Li_2O \rightarrow La_2Li_{0.5}Al_{0.5}O_4 + 1.5LiAlO_2$$

Some authors also hold this viewpoint [9]. It is possible that the lithium aluminate was present in a small amount; therefore, its structure was not visible in the XRD pattern. The $LaAlO_3$ phase

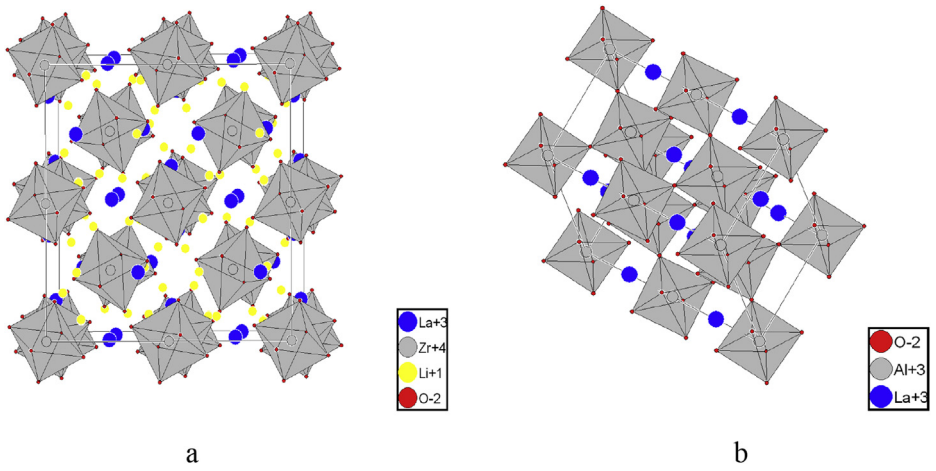

Fig. 2. The structures of LLZ (a) and $LaAlO_3$ (b) constructed according to [1] and [13], respectively.

remains in the samples with Al content greater than 0.20 even after annealing.

The Al-free composition loses lithium because of evaporation of lithium oxide [2]. Then, LLZ partially decomposes with the formation of $La_2Zr_2O_7$ to compensate for the excess of zirconate anions per formula unit of LLZ (with the cation:anion ratio 1:1). The amount of $La_2Zr_2O_7$ decreases with an increase in aluminium doping from 0 to 0.15; therefore, it can be concluded that addition of aluminium weakens the tendency to evaporation of lithium oxide. This effect may be due to more stable bonds Li–O–Al than Li–O–Zr.

The main phase of the Al-containing annealed samples has a cubic structure, type Ia–3d, that corresponds to the literature data [2]. The unit cell parameter a decreases with increasing aluminium content to $x = 0.15$. At further introduction of Al, the parameter a remains almost constant (see Fig. 4). This most likely means that the solid solution reaches saturation at $x = 0.15$. The observed decrease of a can be explained if we suppose that aluminium is in the position of zirconium with a larger ionic radius. Our preliminary experiments on lithium stoichiometry variation in LLZ showed that the cell parameter, according to neutron scattering results, decreases slightly with an increase in lithium concentrations from $Li_7La_3Zr_2O_{12}$ to $Li_9La_3Zr_2O_{13}$ (Fig. 5). Thus, if Al atoms occupy the positions of Li atoms, a large number of lithium vacancies will be formed according to the reaction:

$$3Li_{Li}^{x} + 1/2Al_2O_3 \rightarrow Al_{Li}^{\cdot\cdot} + 2V_{Li}' + 3/2Li_2O.$$

The amount of lithium per formula unit will decrease, leading to an increase in the cell parameter, rather than to its reduction as observed in this work. The detailed investigation of properties $Li_xLa_3Zr_2O_{8.5+0.5x}$ ($x = 7, 8, 9$) including neutron diffraction data will be reported in a separate paper.

Thus, we assume that Al atoms occupy the 16a positions of Ia–3d, which have Zr in undoped LLZ [14]. Moreover, aluminium can occupy also free 16b positions. No exact distribution of aluminium in these positions can be estimated because of a small amount and low scattering power of Al ions compared to Zr ions. Here, the structural analysis is complicated by the presence of additional phases.

3.2. Transport properties

The relative density of the samples increases from 55 to 82% of the theoretical density (5.098 g cm^{-3}, [14]) with an increase of Al, i.e., addition of Al facilitates the process of ceramic sintering. This effect was described elsewhere [9].

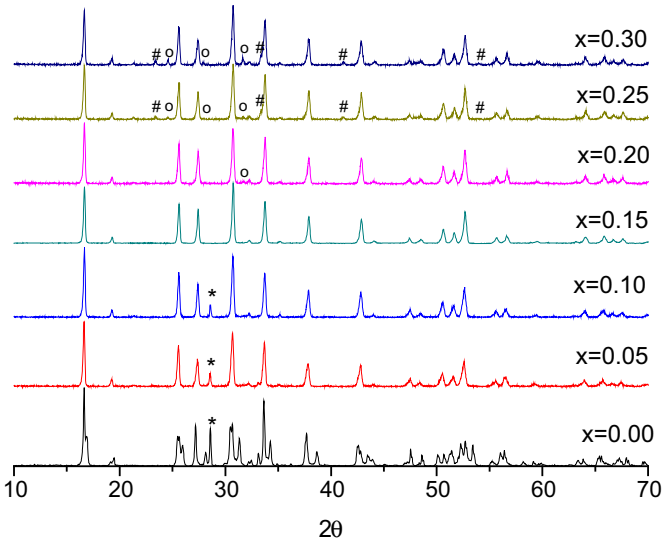

Fig. 3. XRD patterns of annealed samples $Li_7La_3Zr_{2-0.75x}Al_xO_{12}$ ($x = 0.00, 0.05, 0.10, 0.15, 0.20, 0.25, 0.30$) (* – $La_2Zr_2O_7$, # – $LaAlO_3$, o – $La_2Li_{0.5}Al_{0.5}O_4$).

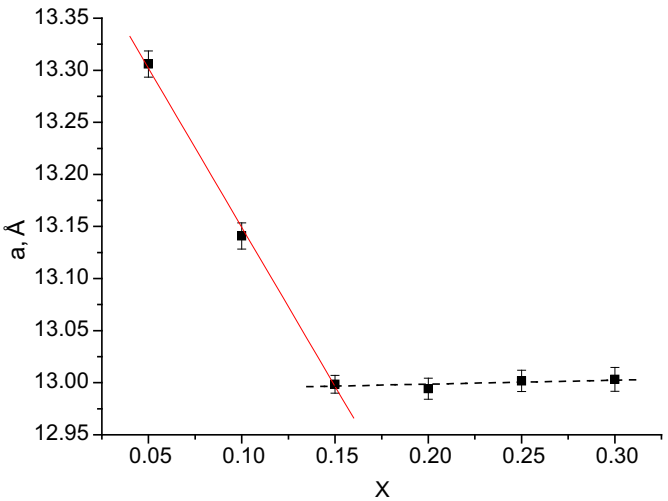

Fig. 4. The parameter a as a function of Al content.

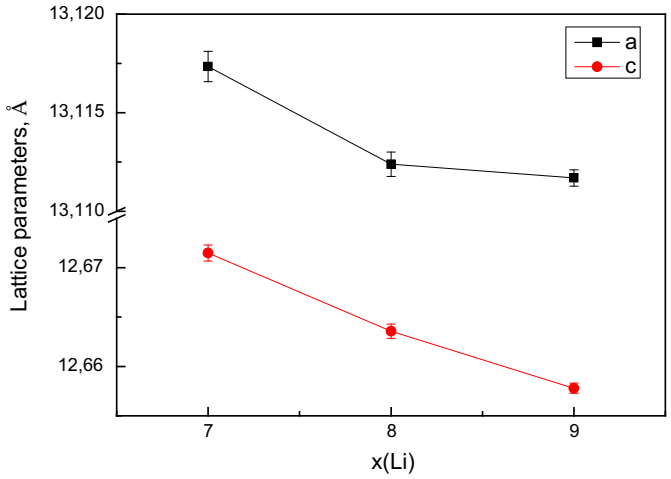

Fig. 5. The parameters *a* and *c* as functions of Li content in $Li_xLa_3Zr_2O_{8.5+0.5x}$.

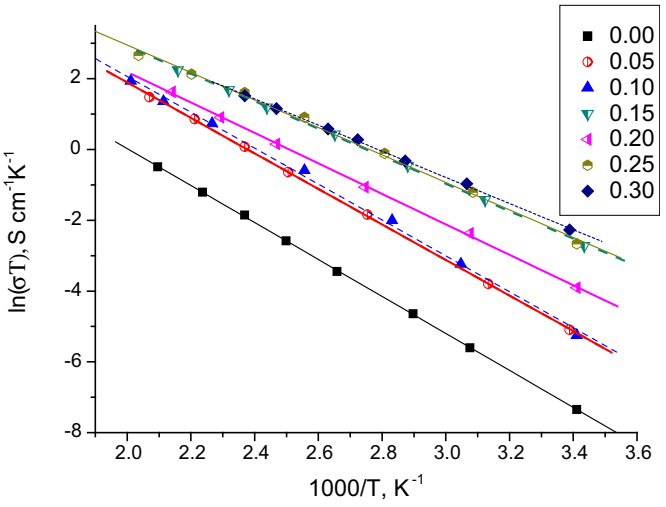

Fig. 7. Arrhenius plots for total conductivity of annealed samples $Li_7La_3Zr_{2-0.75x}Al_xO_{12}$.

Typical impedance plots obtained at room temperature are shown in Fig. 6. For the samples with a small amount of Al, the impedance spectrum at ~25 °C may be separated into two semicircles. In Ref. [2], the high-frequency semicircle can be attributed to the bulk resistance of LLZ, while the semicircle in the low-frequency range correlates with the grain-boundary resistance.

Because at high temperatures or high aluminium concentrations, the impedance plots cannot be resolved into bulk and grain-boundary resistances, we will only discuss the values of total resistance and total conductivity. Fig. 7 displays the temperature dependence of the total conductivity in Arrhenius coordinates. In the examined temperature range, the total conductivity varies linearly with temperature.

The activation energy of conductivity decreases monotonically with an increase in the aluminium content, except for samples with $x = 0.15$ (see Fig. 8). Note that this point corresponds to the unique single-phase composition discussed previously. The differences in the activation energy observed for the other compositions may be caused by some composite effects.

Because the density of all the samples differs from each other, we recalculated the conductivity values to 100% density according to the mixture equation (see our previous work [15]). The dependences of the recalculated conductivity on the Al concentration in $Li_7La_3Zr_{2-0.75x}Al_xO_{12}$ at different temperatures are shown in Fig. 9.

The conductivity rises significantly when the Al content increases from 0.00 to 0.05 as a result of the transition from the tetragonal to cubic LLZ modification. The change in conductivity at $x = 0.15$ is caused by a decrease in the amount of the $La_2Zr_2O_7$ impurity. Then, this impurity disappears and the concentration dependence reaches a plateau x increases. The composition at $x = 0.20$ has a slightly lower conductivity and a higher activation energy, than one at $x = 0.15$. This phenomenon may be related to the formation of small amounts of the impurity phase at the LLZ grain boundaries, which could increase the sample's resistance. At $x > 0.20$ the number of additional phases increases, forming

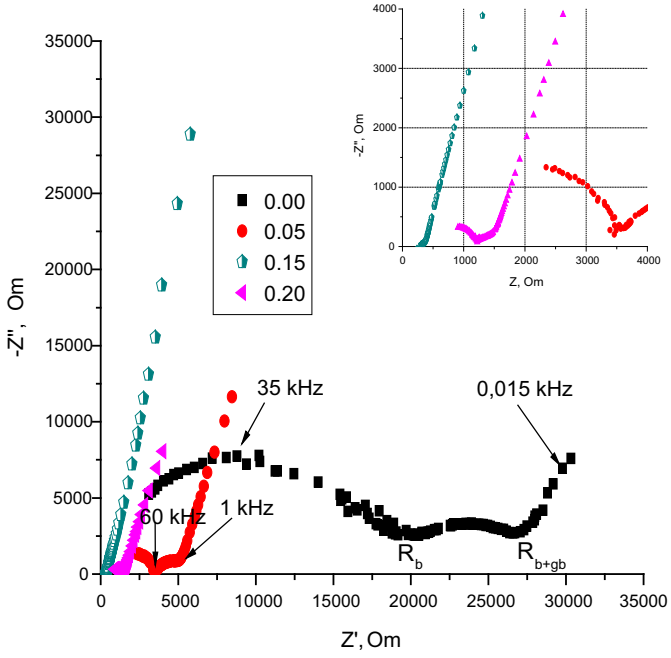

Fig. 6. Impedance plots of annealed samples $Li_7La_3Zr_{2-0.75x}Al_xO_{12}$ ($x = 0.00, 0.05, 0.15, 0.20$) at 25 °C. Inset: high frequency region of the same spectra.

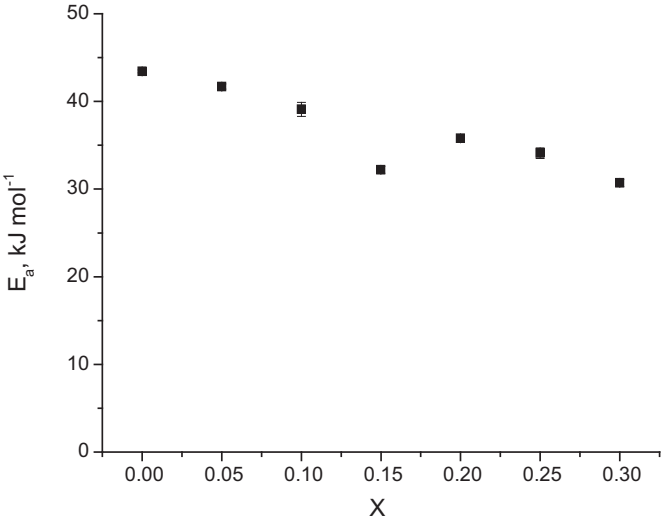

Fig. 8. The activation energy of annealed samples $Li_7La_3Zr_{2-0.75x}Al_xO_{12}$ versus the Al content.

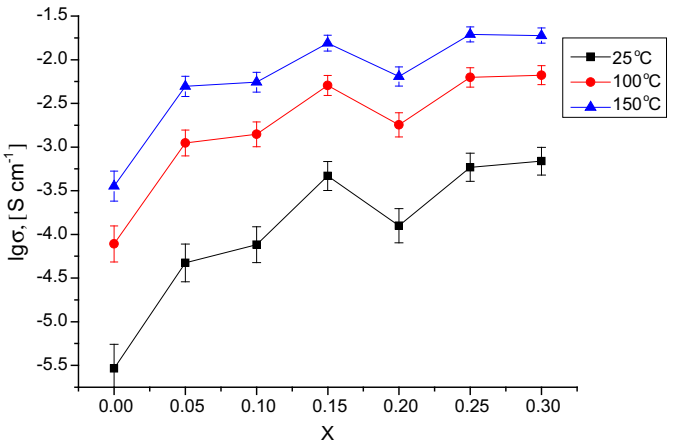

Fig. 9. Concentration dependences of the total conductivity of annealed samples $Li_7La_3Zr_{2-0.75x}Al_xO_{12}$ recalculated to 100% density.

individual isolated particles which do not interrupt the Li-ion motion through the $Li_7La_3Zr_2O_{12}$ phase.

Al doping does not lead to any evident decrease in conductivity over the whole range of formulations investigated. The ion-charge carrier concentration in the superionic phases affects the conductivity more strongly than the vacancy concentration (the concentration of vacancies is high already in structure-disordered phases) [10]. These findings suggest that Al does not substitute for Li ions; otherwise, the Li-ion concentration would decrease significantly in the superionic LLZ phase.

4. Conclusion

The samples of $Li_7La_3Zr_{2-0.75x}Al_xO_{12}$ (x = 0.00, 0.05, 0.10, 0.15, 0.20, 0.25, 0.30) were synthesised by the citrate–nitrate method. It is shown that the substitution of aluminium for zirconium in cation sites facilitates the transition to the cubic modification of LLZ, which has higher conductivity, than its tetragonal form. In our work, the cubic modification of LLZ was obtained by annealing for 1 h at 1150 °C (versus 6 h at 1200 °C in the literature). The composition at $x = 0.15$ is formed without noticeable impurities. Its total conductivity is approximately $3.4 \cdot 10^{-4}$ S cm^{-1} at 25 °C, and its activation energy is 32.2 ± 0.4 kJ mol^{-1}. The lithium garnet $Li_7La_3Zr_{1.89}Al_{0.15}O_{12}$ can be used as a solid ceramic electrolyte for all-solid state lithium rechargeable batteries.

Acknowledgement

We are grateful to Voronin Vladimir Ivanovich for carrying out the neutron scattering experiments.

This work was supported by the program of OHNM RAS “The creation of new metal, ceramic, glass, plastic and composite materials” (project No. 12-T-3-1007 “Relationship of the structure and transport properties of lithium-conducting electrolytes based on $Li_7La_3Zr_2O_{12}$ with trivalent cations (Al, Sc, Y) substituting for zirconium”).

References

[1] J. Awaka, N. Kijima, H. Hayakawa, J. Solid State Chem. 182 (2009) 2046–2052.
[2] R. Murugan, V. Thangadurai, W. Weppner, Angew. Chem. Int. Ed. 46 (2007) 7778–7781.
[3] S. Adams, R.P. Rao, J. Mater. Chem. 22 (2012) 1426–1434.
[4] I. Kokal, M. Somer, P.H.L. Notten, Solid State Ionics 185 (2011) 42–46.
[5] M. Huang, T. Liu, Y. Deng, Solid State Ionics 204–205 (2011) 41–45.
[6] A. Kaeriyama, H. Munakata, K. Kajihara, ECS Trans. 16 (2009) 175–180.
[7] Y. Shimonishi, A. Toda, T. Zhang, Solid State Ionics 183 (2011) 48–53.
[8] S. Kumazaki, Y. Iriyama, K.-H. Kim, R. Murugan, Electrochem. Commun. 13 (2011) 509–512.
[9] Y. Jin, P.J. McGinn, J. Power Sources 196 (2011) 683–687.
[10] A.K. Ivanov-Shits, I.V. Murin, Ionica Tverdogo Tela (Solid State Ionics), vol. 1, S. Petersburg University Press, 2000 (in Russian).
[11] C.A. Geiger, E. Alekseev, B. Lazic, M. Fisch, Inorg. Chem. 50 (2011) 1089–1097.
[12] A. Kuhn, J. Choi, L. Robben, F. Tietz, Z. Phys. Chem. 226 (2012) 525–537.
[13] T. Kojima, K. Nomura, Y. Miyazaki, J. Am. Ceram. Soc. 89 (2006) 3610–3616.
[14] J. Awaka, A. Takashima, K. Kataoka, N. Kijima, Chem. Lett. 40 (2011) 60–62.
[15] E.A. Il'ina, O.L. Andreev, B.D. Antonov, J. Power Sources 201 (2012) 167–173.